A Letters Journal Exploring the Frontiers of Physics

July 2009

EPL, **87** (2009) 17008
doi: 10.1209/0295-5075/87/17008

www.epljournal.org

Current-direction–induced rectification effect on (integer) quantized Hall plateaus

A. Siddiki[(a)]

Physics Department, Arnold Sommerfeld Center for Theoretical Physics, and Center for NanoScience, Ludwig-Maximilans-Universität - Theresienstrasse 37, 80333 Munich, Germany, EU and Physics Department, Faculty of Arts and Sciences - 48170-Kötekli, Muğla, Turkey

received 21 February 2009; accepted in final form 25 June 2009
published online 24 July 2009

PACS 73.43.Cd – Theory and modeling
PACS 73.50.Fq – High-field and nonlinear effects
PACS 73.40.Ei – Rectification

Abstract – Current distribution across narrow Hall bars in out of linear response regime is studied within a self-consistent Hartree-type mean-field approximation for samples which are equally and unequally depleted laterally. The existence of the current-carrying incompressible strips and their influence on magneto-transport properties are investigated. We predict that, the extent and the presence of the quantized Hall plateaus strongly depend on the current direction, in the out of linear response regime, when considering unequally depleted samples. Our magneto-transport results are in contrast to the ones of the conventional theories of the integer quantized Hall effect. We propose certain experimental conditions to test our theoretical predictions at high-mobility, narrow samples.

Surprisingly, open questions remain even nowadays in the theory of the IQHE almost three decades after its discovery [1]. When a two-dimensional electron system (2DES) is subject to a strong perpendicular magnetic B-field, the energy spectrum is (Landau) quantized. Due to the gapped density of states (DOS), the measured longitudinal and Hall resistances, R_L and R_H, respectively, present anomalies if the electron density ($n_{\rm el}$) is an integer multiple of the quantized magnetic flux density (n_ϕ), such that $R_L = 0$ and Hall resistance becomes quantized, *i.e.* $R_H = \frac{e^2}{\nu h}$, where filling factor $\nu (= n_{\rm el}/n_\phi)$ is an integer, e is the electron charge and h is Planck's constant. The IQHE is discussed usually within the bulk [2,3] and the edge [4–6] pictures, which are complementary to each other in describing different experimental results. The bulk picture considers an infinite 2DES within a single-particle approximation and utilizes localization, induced by the disorder, to obtain the essential features of the QHE. However, fails to explain the high reproducibility of the quantized Hall plateaus and to provide computational methods to calculate the magneto-resistance, under experimental conditions. The edge picture relays on the fact that the confining potential bends the Landau levels upwards near the edges of the sample and the edge channels are formed at the Fermi level E_F. The single-particle noninteracting edge theory is known as the Landauer-Büttiker formalism, where the channels are 1D and transport is ballistic, which utilizes the Landauer formalism developed to describe electronic transport at low dimensions without magnetic field and generalizes it in the presence of a perpendicular B-field. The Chklovskii picture is an extension of the Landauer-Büttiker theory including interactions in an *a priori* manner, where the edge channels are no longer 1D and QHE is explained due to the absence of backscattering. Both edge approaches also need localization assumptions to provide realistic magneto-resistance results. The spatial distribution of the externally imposed current, far from the contacts, is discussed within the formation of *compressible* [4,6] or in the *incompressible* [7–10] edge states, which are formed as a direct consequence of Landau quantization and Coulomb interaction. In short, if the Fermi level is pinned locally one of the Landau levels (LLs), due to high DOS, the system behaves like a metal and is called compressible. Otherwise, Fermi level falls in between two consecutive LLs, the system is incompressible pointing that screening is poor.

The local probe experiments provide a strong evidence suggesting that the current is carried by the

(a)E-mail: siddiki@mu.edu.tr

incompressible strips (ISs) [11,12]. In particular, experiments performed at the von Klitzing's group a scanning force microscope was used to measure the spatial distribution of the Hall potential across the 2DES as a function of the B-field [11]. The observed dependence of the Hall potential profiles on ν already suggests the dominant role of the $e-e$ interactions and the existence of ISs in a finite B interval. The measured potential profiles were categorized mainly into three types: type I ($1.6<\nu<2$, out of quantized Hall plateau (QHP)), the potential varies linearly in position similar to classical Hall effect, type II ($\nu\approx 2$, high-field edge of the QHP) non-linear spatial variation, suggesting that the current is confined into the bulk and, type III ($2.05<\nu<2.3$, lower-field side of the QHP), where the potential strongly varies at the edges presenting clear drops, whereas, is constant at the bulk. This sequence of I-II-III is repeated also for higher filling factors, which we show the corresponding results of our calculations in fig. 3.

The main features of the experimental observations were explained within the self-consistent (SC) Thomas-Fermi-Poisson theory of screening [13] plus the local Ohm's law [8], which are also the bases of the present paper. However, the interrelation between the IQHE and the potential profiles was left unresolved. In a subsequent theoretical work [9] it was reported that the Thomas-Fermi approximation (TFA), which surpasses the solution of the Schrödinger equation by assuming the wave functions as $\delta(x-X_0)$ and replaces center coordinate X_0-dependent energy dispersion by the local potential plus Landau energies, leads crucial discrepancies compared to the full SC solution of the Schrödinger and Poisson equations. The most prominent difference between these two approximations is that, the TFA results in artificially narrow ISs compared to the full solution, which is due neglecting the finite extent of the wave functions. In other words, the ISs narrower than the quantum mechanical length scales are smeared out, not surprisingly while TFA becomes questionable at these length scales. The non-existence of the ISs at certain B intervals were reported before [14], however, forgotten for many years. In ref. [9] the effect of the finite extent of the wave functions on the ISs was simulated by a spatial averaging of the local quantities over quantum mechanical length scales such as the Fermi wavelength $\lambda_{\rm F}$ or magnetic length l ($=\sqrt{\hbar/eB}$). We discuss the justification of this spatial averaging over $\lambda_{\rm F}$ later, which enabled them to relax the strict local approximation considering magneto-transport and to lift the artifacts arising from the TFA. The main outcome of this work was to show explicitly that, if there exists an IS somewhere across the sample IQHE is measured, *i.e.* the widths of the quantized Hall plateaus strongly depend on the widths of the ISs. For a complete review of the screening theory, we suggest the reader to check ref. [15]. It is worthwhile to emphasize that the predictions of the screening theory about the nonsymmetric QHPs with respect to the classical Hall resistance depending on the mobility and sample width [16] are confirmed experimentally [17,18].

In this work, we first present our geometry and the related electrostatic problem in the presence of a strong perpendicular magnetic field. Next, we investigate the effect of a large current on the local electron density $n_{\rm el}(x)$ within the local Ohm's law, where the DOS $D(E)$ and the magneto-transport coefficients are obtained from the SC Born approximation [19]. The current density $\mathbf{j}(\mathbf{r})$, $n_{\rm el}(x)$ and magneto-resistances are calculated and compared in the out of linear response regime for equally (generic) and unequally depleted samples, far from the source and drain contacts. At unequally depleted samples, the potential profile is steeper at narrow depleted side (here left), compared to the wider depleted side (right). Therefore, the electron density becomes nonsymmetric with respect to the center of the sample, hence the distribution of the ISs. We show that the IS at the steep edge is narrower than the one at the smoother edge. The effect of nonsymmetric density distribution on measured quantities (R_H and R_L) is utilized as an experimental test. We observe that QHPs are enhanced imposing a certain current direction and shrinks at the other direction. Such a rectification effect is counter intuitive considering the conventional theories of QHE, both bulk and the edge, since the extend of the QHPs mainly depend on the mobility at fixed temperature and current amplitude, not its direction.

Here we follow the path of ref. [9] in describing our 2DES implementing the historical Chklovskii geometry [6], *i.e.* a translation invariance in y-(current) direction with two in-plane side gates. However, different boundary conditions [20] and system geometries [21] can be used and are shown to lead similar electrostatic results. The donor density n_0 is assumed to be homogeneous residing together with the electron layer on the $z=0$ plane. The 2DES is depleted from the edges by applying V_L and V_R to the metallic gates on sides. In the screening theory of the IQHE, the Coulomb interaction is included to a spinless single-particle Hamiltonian, within a Hartree-type approximation, via adding an effective mean-field potential (energy) given by

$$V_H(x)=\frac{2e^2}{\kappa}\int_{-d}^{d} n_{\rm el}(t)K(x,t)\mathrm{d}t, \tag{1}$$

where κ is an average dielectric constant ($=12.4$ for GaAs) at the interface of the 2DES and the kernel $K(x,t)$ preserves the boundary conditions $V(-d)=V_L$ and $V(d)=V_R$ for the above described model. The total potential energy is then

$$V(x)=V_{bg}(x)+V_G(x)+V_H(x), \tag{2}$$

where $V_{bg}(x)$ is the background potential generated by the donors and $V_G(x)$ by the gates for a sample width of $2d$. To calculate the Hartree potential, one needs the electron

density distribution, which is given within TFA by

$$n_{\rm el}(x) = \int {\rm d}E D(E) \left[e^{\frac{(E-\mu^*(x))}{k_B T}} + 1 \right]^{-1}, \qquad (3)$$

where k_B is the Boltzmann constant, T the temperature, $\mu^*(x) = \mu^*_{\rm eq} - V(x)$ the electrochemical potential and $\mu^*_{\rm eq}$ the chemical potential at equilibrium. We define the widths of the broadened LLs Γ from the mobility-dependent short-range scattering [9,19]. The SC scheme is closed by eqs. (2) and (3) provided that the left and right depletion lengths, b_l and b_r, are given. The numerical task is now to solve these equations by iteration until the electron density distribution remains unchanged up to a numerical accuracy of 10^{-8}. Next, the local current density $\mathbf{j}(\mathbf{r})$ is calculated assuming a fixed current in the y-direction $I = \int_{-d}^{d} j_y(x,y){\rm d}x$ via (local) Ohm's law

$$\boldsymbol{\nabla}\mu^*(\mathbf{r})/\mathbf{e} \equiv \mathbf{E}(\mathbf{r}) = \hat{\rho}(\mathbf{r})\mathbf{j}(\mathbf{r}), \qquad (4)$$

provided that the resistivity tensor $\hat{\rho}(\mathbf{r})$ is known through the DOS [8,9] and assuming a stationary state using the local electric field $\mathbf{E}(\mathbf{r})$ obtained in the previous step. The translation invariance is utilized together with the equation of continuity $\boldsymbol{\nabla}\cdot\mathbf{j}(\mathbf{r}) = \mathbf{0}$ and $\boldsymbol{\nabla}\times\mathbf{E}(\mathbf{r}) = \mathbf{0}$ to obtain

$$\begin{aligned} j_x \equiv 0, \qquad & E_y(x) \equiv E_y^0, \\ j_y(x) = E_y^0/\rho_L(x), \qquad & E_x(x) = E_y^0 \rho_H(x)/\rho_L(x), \end{aligned} \qquad (5)$$

where $\rho_L(x)$ and $\rho_H(x)$ are the diagonal and off-diagonal entries of the resistivity tensor, respectively, and the constant electric field in the y-direction $E_y^0 = I.\left[\int_{-d}^{d} \frac{{\rm d}x}{\rho_L(x)}\right]^{-1}$. Then $\mu^*(x)$ is obtained from eq. (4) by integration, up to a constant which is fixed by $n_{\rm el}$. The numerical scheme is initialized with $n_{\rm el}(x)$ calculated without current, afterwards calculate the current distribution for a given fixed I. Next, we obtain $\mu^*(x)$ such that $n_{\rm el}$ is kept constant and start the new iteration from the newly calculated $n_{\rm el}(x)$. This procedure is continued until convergence is obtained. Here, we apply the above described scheme to an unequally depleted gate defined sample. Likewise in ref. [9], we perform a spatial averaging over $\lambda_{\rm F}$ ($\sim 33\,$nm) to simulate the effects of the finite extend of the wave functions, which also lifts the strict locality of the Ohm's law. Recent analytical calculations including higher order contributions to the local conductivity tensor [22] provide a firm ground to make such an averaging in our theory. At this point we clarify our assumptions about the injection and probe contacts. It is well known that the current within the ISs is divergent free [16] and the current cannot be injected directly to them, therefore, the current is first injected to the compressible regions from the (injection) contacts. Since there is an electrostatic field parallel to the boundary between compressible and incompressible strip, there will be a Hall current crossing this boundary due to the change in Hall conductivity across the boundary then imposed current is confined to the ISs. Similarly, impurity scattering may play a role with a less pronounced importance, which is included implicitly when calculating the conductivity tensor elements from the SC Born approximation. The explicit treatment of the contacts is a formidable task [23] and is beyond the scope of the present paper. Since we perform our calculations sufficiently faraway from the source and drain contacts hence can avoid such a complicated treatment. Considering the probe contacts, one measures the difference of the electrochemical potential on the two edges of the Hall bar. In our scheme, we start with a constant (position-independent) electrochemical potential in equilibrium and by solving the self-consistent set of equations considering electrostatics and local Ohm's law, and obtain a position-dependent electrochemical potential, which results in a difference between the two edges of the Hall bar. Another important assumption of our model is to perform an spatial averaging over $\lambda_{\rm F}$, the full Hartree calculations explicitly show that if the width of the IS becomes comparable with the extend of the wave function, *i.e.* $\sim\sqrt{2}l$, the IS vanishes. Moreover, due to scattering the overlap of the wave functions become large and the IS becomes "leaky" even on these length scales. For a comparison at 5 T the extend of the wave function is $\sim$20 nm, which is at the same order as $\lambda_{\rm F} \sim 25$–$35\,$nm for typical samples. Also note that, we are dealing with a thermodynamic ensemble, *i.e.* we utilize the Fermi-Dirac distribution, which makes sense only if there are sufficient number of particles within the considered spatial region. This also sets a constriction on the length scales related to the mean particle distance, *i.e.* Fermi wavelength, where one can perform reliable calculations.

It is known that the large current, *i.e.* out of linear response regime, induces an asymmetry on the widths of the ISs [8,10], which is also observed experimentally [24]. This due to the tilting of the LLs as a result of self-consistency, *i.e.* adding the Hall potential to the total potential and recalculating the electron density. The slope of the Hall potential is determined by the current direction and its amplitude, thereby the tilting angle of the LLs. To avoid any confusion we use the word *asymmetric* to denote the effect of imposed current and *nonsymmetric* for the effect of unequal depletion on the density or IS distributions. Our aim is, first to present this current-induced asymmetry calculated for an equally (and widely) depleted sample from both edges. Next using the side gates, we deplete the sample unequally such that the potential on the right hand side (RHS) is smoother than that of the left hand side (LHS). Hence, the IS on RHS is larger even without any current-induced effect. Finally, we apply large negative ($-$) and positive ($+$) DC currents to the system and investigate its effect on the density distribution and the widths of the QHPs.

In our calculations, the current amplitude is sufficiently large being in the out of linear response regime ($I \sim 3\,\mu$A). As a consequence of a ($+$) bias, if there is an IS, the spatial

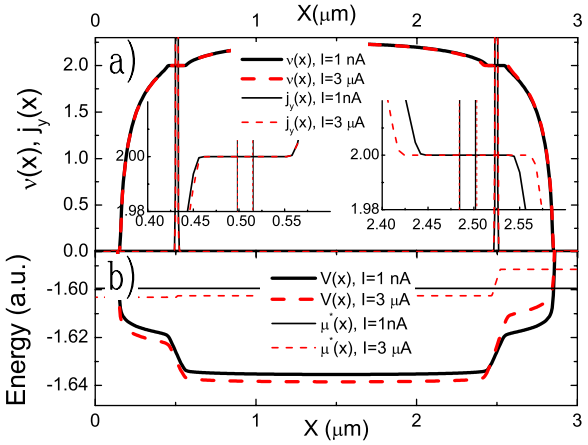

Fig. 1: (Color online) (a) The spatial distribution of $\nu(x)$ and the corresponding $j_y(x)$ considering a generic (symmetric, *i.e.* $b_l = b_r = 150\,\mathrm{nm}$, assuming $V_L = V_R = 0$) $3\,\mu\mathrm{m}$ sample. (b) The SC and electrochemical potentials under low (solid lines) and high bias (broken lines). All calculations are done for $\hbar(eB/m)/E_F^0(=\Omega/E_F^0) = 0.94$, where E_F^0 $(= 12.75\,\mathrm{meV})$ is the Fermi energy at the center, *i.e.* $X = 1.5\,\mu\mathrm{m}$, at the default temperature $k_BT/\Omega = 0.025$. A homogeneous donor density of $n_0 = 4\times10^{11}\,\mathrm{cm}^{-2}$ is assumed, with the impurity parameter $\Gamma/\Omega = 0.03$.

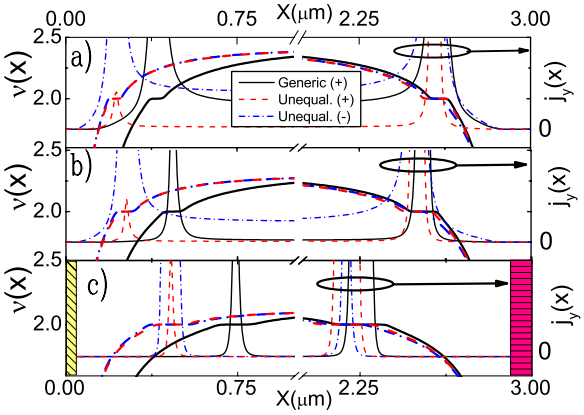

Fig. 2: (Color online) The local variation of the filling factor and the current densities for three selected B values, indicated in fig. 4, considering: i) a generic sample (black solid line) and ii) an unequally depleted sample, by setting $V_L = 0$ and $V_R = -1.1\,\mathrm{V}$ which results in $b_l = b_r/2 = 75\,\mathrm{nm}$. Current directions are indicated by (red) broken lines for (+) and (blue) dash-dotted lines for (−) bias. The unequal depletion is shown by the diagonal shaded region on LHS and horizontal shaded region on RHS (c), which lead $E_F^0 = 13.12\,\mathrm{meV}$.

extend of the (energy) gapped region on the RHS becomes wider, whereas shrinks on the LHS, resulting in a wider IS on the RHS and a narrower IS on the LHS. Such a situation is shown in fig. 1a for the generic sample, which will be positively biased throughout the paper. The local electron density distributions (or equivalently the local filling factor $\nu(x) = 2\pi l^2 n_{\mathrm{el}}(x)$) calculated at low (thick solid lines) and high (thick broken lines) current biases are shown together with the current density distribution (thin vertical lines) in the upper panel. Clearly, the IS on the RHS is larger than the one on the LHS under the large current bias (cf. the inset of fig. 1) and the current (horizontal lines) is well confined to the ISs. Figure 1b presents the SC potentials (thick lines) together with the position-dependent electrochemical potentials (thin lines). We observe that at the large bias the Hall potential tilts the total potential, hence the LLs. Since, the compressible regions can almost perfectly screen the Hall potential, we see that the major effect on the $\mu^*(x)$ is observed at the regions where an IS resides.

Further, we investigate the effect of current-bias–induced density asymmetry at the unequally depleted samples. In fig. 2 (black) solid curves present $\nu(x)$ of a generic sample. For the lowest B value (a), no ISs exist larger than λ_{F} for the generic and negatively biased unequally depleted samples (dash-dotted (blue) lines). Therefore, the electron and the current densities both remain symmetric (the system is completely compressible), hence the induced Hall potential can be almost perfectly screened. The current distribution exhibits, local peaks at the positions of $\nu(x) \approx 2$, where $\rho_L(x)$ takes small values in the very close vicinity of $\nu(x) = 2$, although no IS exists. One can see that some amount of current is still flowing from the bulk for these cases, *i.e.* generic and unequally depleted sample with (−) bias. However, for the unequally depleted sample under (+) bias (broken (red) lines) the IS on the RHS is larger than λ_{F} and the current is confined within this region mainly and no current flows from the bulk. We observe that for this B value, the generic sample under (+) bias and unequally depleted sample under (−) bias are out of the QHP, *i.e.* no ISs exist across the samples. Increasing B slightly (fig. 2b), an IS develops on the RHS of the generic sample where most of the current is confined to. Meanwhile on the LHS, due to the local minima mentioned before, a small amount of current also flows. Interestingly, at this B value no current flows from the bulk (up to our numerical accuracy, *i.e.*, $10^{-14}\,\mathrm{A}$) and the system is in a QHP both for generic and unequally depleted positively biased samples. Increasing the B-field furthermore, leads formation of an IS also at the unequally depleted sample under (−) bias, hence all three samples are in the plateau regime. When the center ν becomes equal to two (not shown here) the *two* edge ISs merge at the bulk and all the current flows from the *incompressible bulk*, slightly asymmetric with respect to the center. At the highest B-field strengths shown in fig. 4, the system is out of the QHP and both the electron and the current densities become symmetric, again.

Next, we analyze the calculated Hall potential profiles in terms of Ahlswede experiments [11]. In fig. 3 the sequence of the potential types, calculated at six B values with equal steps of $0.05\,\Omega/E_F^0$ (starting from 0.8) for different samples are shown. Our results for the generic sample in the out of linear response regime coincides with the experimental findings [11], where to obtain a clear voltage signal a relatively high current is imposed and as a

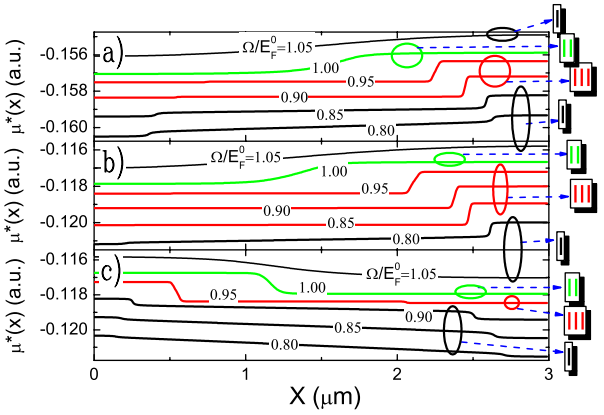

Fig. 3: (Color online) Position-dependent electrochemical potentials calculated at characteristic B values for: a) generic, b) and c) unequally depleted samples under positive (a, b) and negative (c) bias. The potential types are indicated by I, II and III (and also by color code), each calculated profile is shifted in energy by a small amount ($\Delta = 0.001\Omega/E_F^0$) for clarity.

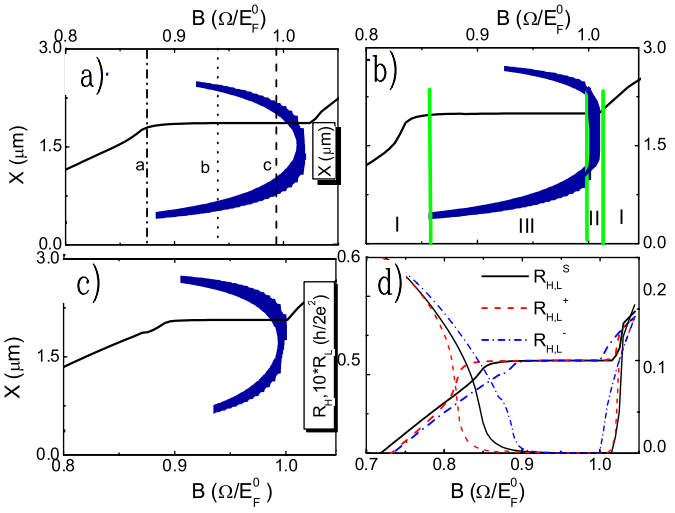

Fig. 4: (Color online) The spatial distribution of the ISs (blue regions) as a function of B together with calculated R_H (black solid line) for generic (a) and unequally depleted samples with positive (b) and negative (c) DC current. (d) The corresponding R_H and R_L. Vertical lines indicate the B-field values shown in fig. 2.

consequence asymmetric potential drops were observed at the edges. The sequences of potential profiles we observe are: I-I-III-III-II-I for the generic sample, for the unequally depleted samples, I-III-III-III-II-I at (+) bias and I-I-I-III-II-I at the (−) negative bias. It was stated that [11], if the Hall potential is linear the system is out of the QHP (classical Hall effect), both experimentally [11] and theoretically [16]. Therefore we would expect that the unequally depleted sample under (+) bias remains in the plateau for the largest B interval, whereas same sample under (−) bias should present the narrowest plateau. This is somehow easy to understand, if one starts already with an nonsymmetric density profile, the asymmetry induced by the large current will be either enhanced or suppressed depending on the current direction. A (+) bias will tilt the LLs resulting a high potential on the RHS as in fig. 3a and 3b, whereas a (−) bias will do the opposite, 3c. Therefore, for the (+) bias the IS on the RHS becomes wider, which essentially means that the unequally depleted sample enters to the QHP at a lower B-field compared to a generic sample and (−)-biased ones, due to already existing large IS at the RHS. The situation is rather different for the (−) bias, since the narrow IS is on the LHS and the high bias will enlarge this IS. Hence, there is a competition between the slope of induced Hall potential and the confinement, and thereby screened, potential to generate a wide IS. Thus, the unequally depleted sample when (−)-biased will enter to the QHP at a higher B-field value compared to both (+)-biased and generic samples. Our findings suggest that, if the Hall potential profiles are measured by the scanning force microscopy setup considering unequally depleted samples, the sequence of the potential types will alter at the lower B-field side of the QHP under (+) and (−) current bias.

Finally we investigate the magneto-resistance quantities of the systems under consideration. As mentioned above, the extend of the QHPs depend strongly on the density asymmetry and the current direction. Figure 4 summarizes our main findings, where we show the calculated Hall and longitudinal resistances obtained from our self-consistent scheme, together with the positions and the widths of ISs with $\nu(x) = 2$ at the background. We only depict the ISs wider than λ_F with dark (blue) regions, whereas if the electrons reside in a compressible region it is colored by white areas. Figure 4a presents the evolution of the ISs as a function of the B-field for a generic sample under (+) current with an amplitude of $3\,\mu$A. To clarify the color code we suggest the reader to compare the positions of the ISs with fig. 2 along the lines denoted by a, b and c. As soon as an IS formed ($B \sim 0.88$) at the lower edge of the sample ($x \sim 0.5\,\mu$m) the system is in the QH regime. As an important note, it is sufficient to have *only one* incompressible strip to observe quantized Hall effect. This is in contrast to many-edge channel theories [5,6]. However, such an effect is already known as the cold edge by the experimentalists [25]. In the out of linear response regime, the R_L is measured only from one side of the sample, since backscattering takes place on the other side (the IS is smeared out, the hot edge) and R_L never vanishes as a consequence of the density asymmetry induced by the large current. We should also mention that such a situation cannot be handled by perturbation methods [22] (or like Kubo formalism) without self-consistency. The Hall resistances and the distribution of ISs for unequally depleted samples are shown in fig. 4b and c. It is observed that the current direction affects the widths of the ISs, hence, the extend of the QHPs. The large (+) bias enlarges the already wide IS on the RHS which leads an extended QHP, whereas (−) bias results in the opposite.

Let us discuss the experimental conditions to investigate the predicted rectification effect. First of all, the Hall bars should be defined on high-mobility ($\geqslant 1.0 \times 10^6\,\mathrm{cm}^2\,\mathrm{V/s}$) and narrow ($2d \lesssim 10\,\mu\mathrm{m}$) unequally depleted samples. One possible option is to define the Hall bars similar to the ones investigated in ref. [17,18], at which an asymmetry in R_L, concerning probe sides, is observed. The preliminary experimental findings measured at these samples provide a clear signature of the predicted rectification. The main drawback of the gate defined samples relies on the fact that, using gates one cannot create very steep edge potential profiles, therefore, rectification may be somewhat suppressed. Meanwhile, one can define Hall bars with steeper edge potentials by deep etching, of course, with different etching dept on both sides. However, it is known that etching can cause inhomogeneities at the density profile which may become important when considering narrow samples. A hybrid solution, *i.e.* one side etched, other side gate defined, seems to be the most reasonable solution. To obtain the extreme sharp edge on one side, it is desirable to perform the suggested experiments on cleaved edge overgrown (CEO) samples, where it has been shown that no ISs reside at the sharp edge [26]. The experiments need not to be done at very low temperatures ($0.4 < T < 4.0\,\mathrm{K}$), whereas the imposed current should not exceed the breakdown current due to Joule heating [10], which can easily be determined by the experiments.

In conclusion, we utilized the SC calculation scheme developed by R. R. Gerhardts and his co-workers to obtain the electron density and magneto-resistance properties of equally and unequally depleted samples, *i.e.* in the presence of an asymmetric lateral confinement. Noticeably, our theory does not involve the localization of the wave functions which was the main-stream idea of the QHE for two decades, which fails to provide an explicit calculation scheme to obtain magneto-resistances under experimental conditions. Strikingly we observe that it is sufficient to have only *one edge incompressible strip* to measure quantized Hall resistance, which is also in contrast to other edge-channel theories.

For the high-mobility, narrow and unequally depleted samples we predict that, the large current either enlarges or shrinks the QHPs depending on whether the asymmetry induced by the current and the nonsymmetric density distribution caused by the edge profile are in the same direction or not. Based on our findings, we proposed three sets of sample structures where the effect of the current-induced asymmetry and thereby the rectification of the QHPs can be controllably measured. We expect that, the rectification effect will be even enhanced due to the Joule heating at such high currents, since the narrow ISs will be smeared out easily. Beyond the breakdown current the current direction will be unimportant, while no ISs exists. Moreover, we also predict that the Hall potential profile types at the lower edge of the Hall plateau will be altered if scanned by force microscopy techniques concerning the unequally depleted samples.

* * *

The author would like to thank M. Grayson for invaluable discussions concerning the CEO samples, J. Horas, D. Kupidura and S. Ludwig for the gate defined samples, R. R. Gerhardts and K. Güven for initiating and developing the screening theory. This work was financially supported by DIP, NIM Area A and SFB 631.

REFERENCES

[1] v. Klitzing K., Dorda G. and Pepper M., *Phys. Rev. Lett.*, **45** (1980) 494.
[2] Laughlin R. B., *Phys. Rev. B*, **23** (1981) 5632.
[3] Kramer B., Kettemann S. and Ohtsuki T., *Physica E*, **20** (2003) 172.
[4] Halperin B. I., *Phys. Rev. B*, **25** (1982) 2185.
[5] Büttiker M., *Phys. Rev. Lett.*, **57** (1986) 1761.
[6] Chklovskii D. B., Shklovskii B. I. and Glazman L. I., *Phys. Rev. B*, **46** (1992) 4026.
[7] Chang A. M., *Solid State Commun.*, **74** (1990) 871.
[8] Güven K. and Gerhardts R. R., *Phys. Rev. B*, **67** (2003) 115327.
[9] Siddiki A. and Gerhardts R. R., *Phys. Rev. B*, **70** (2004) 195335.
[10] Kanamaru S., Suzuuara H. and Akera H., *J. Phys. Soc. Jpn.*, **75** (2006).
[11] Ahlswede E., Weitz P., Weis J., von Klitzing K. and Eberl K., *Physica B*, **298** (2001) 562.
[12] Ilani S., Martin J., Teitelbaum E., Smet J. H., Mahalu D., Umansky V. and Yacoby A., *Nature*, **427** (2004) 328.
[13] Lier K. and Gerhardts R. R., *Phys. Rev. B*, **50** (1994) 7757.
[14] Suzuki T. and Ando T., *J. Phys. Soc. Jpn.*, **62** (1993) 2986.
[15] Gerhartds R. R., *Phys. Status Solidi b*, **245** (2008) 378.
[16] Siddiki A. and Gerhardts R. R., *Int. J. Mod. Phys. B*, **21** (2007) 1362.
[17] Horas J., Siddiki A., Moser J., Wegscheider W. and Ludwig S., *Physica E: Low-Dimens. Syst. Nanostruct.*, **40** (2008) 1130.
[18] Siddiki A., Horas J., Moser J., Wegscheider W. and Ludwig S., arxiv:0905.0204v1 [cond-mat.mes-hall] (2009).
[19] Ando T., Fowler A. B. and Stern F., *Rev. Mod. Phys.*, **54** (1982) 437.
[20] Siddiki A. and Gerhardts R. R., *Phys. Rev. B*, **68** (2003) 125315.
[21] Siddiki A., *Phys. Rev. B*, **75** (2007) 155311.
[22] Champel T., Florens S. and Canet L., *Phys. Rev. B*, **78** (2008) 125302.
[23] Tung R. T., *Phys. Rev. B*, **64** (2001) 205310.
[24] Ahlswede E., Weis J., von Klitzing K. and Eberl K., *Physica E*, **12** (2002) 165.
[25] Heiblum M., private communication.
[26] Huber M., Grayson M., Rother M., Biberacher W., Wegscheider W. and Abstreiter G., *Phys. Rev. Lett.*, **94** (2005) 016805.